PAPER • **OPEN ACCESS**

Experimental investigation of recirculation zone characteristics of a pre-filming airblast injector

To cite this article: N Darwish *et al* 2021 *IOP Conf. Ser.: Mater. Sci. Eng.* **1172** 012046

Experimental investigation of recirculation zone characteristics of a pre-filming airblast injector

N Darwish[1], K P Shanmugadas[2]and S R Chakravarthy[2]

[1] University of Science and Technology at Zewail City, Giza, Egypt
[2] National Centre for Combustion Research and Development & Department of Aerospace Engineering, Indian Institute of Technology Madras, Chennai, India

Email: s-mohammednady@zewailcity.edu.eg

Abstract. The toroidal flow at the recirculation zone has a vital role in combustion process as it helps in mixing hot combustion products with incoming fresh air and fuel which increases combustion efficiency. In the present work, characteristics of recirculation zone are investigated using a pre-filming airblast injector. Particle Image Velocimetry is used to characterize the swirl flow field generated by the airblast injector. Moreover, olive oil is used as a tracer to be captured by a high-speed camera. Different flow rates are investigated in order for finding out the effect of varying flow rates on the characteristics of the recirculation zone. Results for recirculation zone shape, velocity field and shear strength at the primary zone of combustion are represented. Additionally, results show that recirculation zone is almost symmetrical with increasing trend in shear strength with increasing flow rates.

1. Introduction

An increasing demand for better combustion performance from the perspective of decreasing pollutants emissions and increasing combustion efficiency was raised in the recent decades in order to fulfil the firm regulatory requirements [1], [2]. Most of gas turbine systems utilize swirl injectors that create Central Toroidal Recirculation Zone (CTRZ) in the primary combustion region downstream the exit of the injector [3]. The CTRZ plays a vital role in flame stabilization and increasing combustion efficiency as it affords an appropriate forward flow speed that matches with flame speed which aids in flame holding [4]. Moreover, CTRZ creates a region of high shear and strong turbulence that promotes rapid mixing and heat transfer between hot combustion products and fresh incoming air and fuel which improves the combustion efficiency [5]. In addition to this, a flow characteristic that is of significant importance of a swirl injector is the vortex breakdown [6]. It can be identified as a sudden change in the centre of a thin vortex and in most cases it develops into a recirculating spiral pattern forming the CTRZ [7]. Also, it is characterized by a low static pressure in the central core downstream the injector resulting in recirculating the flow [8]. Besides, the flow within the core of the CTRZ has a reverse axial velocity component with no tangential or radial velocity components [9]. Reddy [10] reported a decrease in the tangential velocity along the flow path and the flow transitioned to an axial flow with vanishing tangential and radial components.

Numerical and experimental investigations by Lilley and Gupta [11] (1984) led to identify a term, Swirl Number (SN) for measuring the strength of swirl. SN is the ratio between the axial flux of angular

momentum to the axial flux of axial momentum, studied at the exit of the injector. Additionally, Chigier & Beer [12] (1972) concluded that when the swirl number is around 0.5 ~ 0.6, the swirling motion starts to induce radial and axial pressure gradients in the flow field and when the adverse pressure gradient at the centre of the axis is large enough, CTRZ is formed. Furthermore, Tangirala [13] examined the effect the of swirl numbers by investigating the advantages and drawbacks of high swirl operations. The main result was that when increasing the SN, the mixing and flame stability is enhanced for values approximately till 1 and beyond that value turbulence levels and flame stability are reduced. The main drawback of excessive swirl is that it causes excessive wall heating due to forcing the flame to move upstream getting closer to the wall. Besides, Lu X [14] (2005) carried out a large-eddy simulation analysis to study the vortex breakdown in a coaxial swirl injector. It was concluded that for low swirl number, SN=0.3, vortex breakdown was not observed, however, for SN=0.5, a vortex breakdown was observed resulting in forming a CTRZ.

Chieger & Beer [12] (1972) investigated the types of devices for achieving swirling flows and categorized them as; mechanically rotating vanes with tangential entry of fluid into an axial flow tube called radial swirler and angled vanes in axial flow tube called axial swirler. Moreover, Candel [15] (2014) found that the flame dynamics and the topology of the spray flow field are mainly affected by the size of the CTRZ which is influenced by some geometrical parameters. In addition to, Kilik [16] stated that an enhancement of the size of the CTRZ is achieved by increasing the vane outlet angle. Moreover, a stronger and larger CTRZ is achieved by increasing the curvature of the vanes which minimizes the pressure loss in the swirler compared to a flat axial swirler having the same vanes outlet angle. Also, Beer and Syred [17] (1974) concluded that swirls through enhancing the flow mixing on CTRZ boundaries can reduce the combustion length.

Hadef and Lenze [18] (2008) examined the effect on spray characteristics for different relative swirl rotations of flow, co and counter swirlers. They reported that flame stability was enhanced using counter rotating swirler due to the finer atomization achieved by it. Additionally, Wang [19] reported that the counter-rotating configuration is more preferable than the co-rotating one as the counter-rotating arrangement helps in the formation of fine droplets. Moreover, a drawback of the co-rotating arrangement is that it produces a large recirculation zone leading to a more susceptibility to flame oscillation. Besides, Merkle [20] reported that in the case of a counter-rotating arrangement, more mass flow rate was recirculated in addition to a shorter axial length of the CTRZ in comparing with the co-rotating arrangement.

Fuel atomizers are devices used for spreading liquid fuel to thinnest possible sheet and to atomize it, using the aerodynamic forces generated from swirling flows, into fine droplets [19]. Most modern gas turbine combustors achieve fuel atomization either using an airblast atomizer or using a pressure atomizer [21]. In addition, airblast atomizers are more preferable to be used when a reduction in soot formation and low pollutant emissions are desirable [22]. Furthermore, the atomization process consists of a primary break up and a secondary breakup. During the primary breakup shear force plays a vital role in breaking liquid films into liquid ligaments while through the secondary breakup surface tension works on breaking liquid ligaments into droplets [23]. Additionally, Lefebvre and Rizkalla [24], [25] studied the effects of both liquid and air properties on atomization quality and reported that atomization quality decreases with increasing liquid-air mass ration and with increasing liquid viscosity as liquid films get thicker. In contrast, increasing air velocity and air density accomplishes better atomization.

2. Experimental Procedures

In the present work, Particle Image Velocimetry (PIV) is used to investigate the swirl flow field generated by a pre-filming airblast injector fitted into a vertical chamber to study characteristics such as shear regions, CTRZ shape and velocity components and the effect of varying only inlet air mass flow

rates on these characteristics. Olive oil is used as the tracer particle and SN for inner and outer swirlers are 0.6 and 1.6 respectively.

2.1. Pre-filming airblast injector

The injector used in the present work is a piloted pre-filming airblast injector. The geometry of a pre-filming airblast injector is in figure 1 and more information can be found in [26]. The injector consists of primary and secondary swirlers and a curved pre-filmer called the venture. A dual orifice nozzle is used as the pilot nozzle. The dual orifice fuel nozzle has two fuel circuits: a central primary nozzle that forms a narrow hollow cone spray and a secondary orifice surrounding the nozzle at the centre. The central nozzle creates a primary spray, which is atomized by the primary and secondary air swirl. The secondary orifice spray and part of the primary spray are made to impinge on the venture and proceed with pre-filming airblast atomization [26].

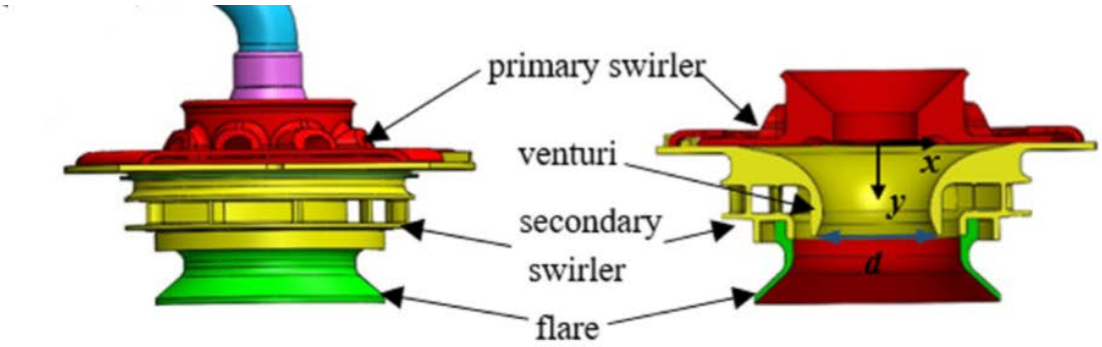

Figure 1. Geometry of a pre-filming airblast injector [26]

2.2. Test conditions

Six different air mass flow rates at room temperature are investigated as tabulated in table 1 along with the bulk velocity at injector exit and Reynolds number associated with each case. Mass flow rates are normalized to the highest used value which is 1512 standard litre per minute (SLPM) for case 6. In addition, bulk velocities are normalized to the highest value which is 9 m/s for case 6.

Table 1. Flow characteristics for different test cases.

	Air mass flow rate	Bulk velocity	Reynolds number
Case 1	0.48	0.48	$2.14*10^4$
Case 2	0.58	0.58	$2.58*10^4$
Case 3	0.64	0.64	$2.845*10^4$
Case 4	0.72	0.72	$3.215*10^4$
Case 5	0.83	0.83	$3.71*10^4$
Case 6	1	1	$4.5*10^4$

2.3. Particle Image Velocimetry and tracer particles

PIV is used to capture the flow field of the seeded air flow downstream the injector. It is based on adding tracer particles to a fluid flow and considering the principle that tracer particles follow fluid flow particles so its motion can be considered as the fluid flow motion. Thereafter, photographing the system twice within a short time interval to capture the displacement moved by the tracer particles. After that by comparing the positions of the same tracer particle at the two different instants of time, the displacement and velocity vectors of the fluid flow can be calculated. The difference between the two shots of laser could be around 40 microsecond.

Moreover, the tracer particles should be small enough to follow the flow and at the same time have correct density and good dispersion of light. A balance has to be achieved between these sides during the experiment [27]. A commonly used tracer particles are oil particles which are prepared by injecting air at high pressures into the oil via a number of nozzles. Each nozzle consists of a tube with a number of small holes in them. Hence, each nozzle produces micro-bubbles with micro-droplets inside. When these bubbles reach the oil surface they burst releasing these droplets. Internal baffles are used to remove the larger unwanted particles. Density of seeding is determined by the air flow and number of nozzles that's why seeding density can be controlled by altering the air flow to the nozzles or by turning one or more of the nozzles on or off [28].

For the present experiment, an ND: YLF Litron laser is used synchronized with one Photron high speed camera with adapters. The acquired pictures are processed using the commercial software Davis. More than 6000 pictures are used for processing of each measurement. An example of similar setup arrangement is shown in figure 2 noting that for the present experiment only one camera is used. Furthermore, Olive oil was used for this experiment for its good characteristics that meet the mentioned requirements [29].

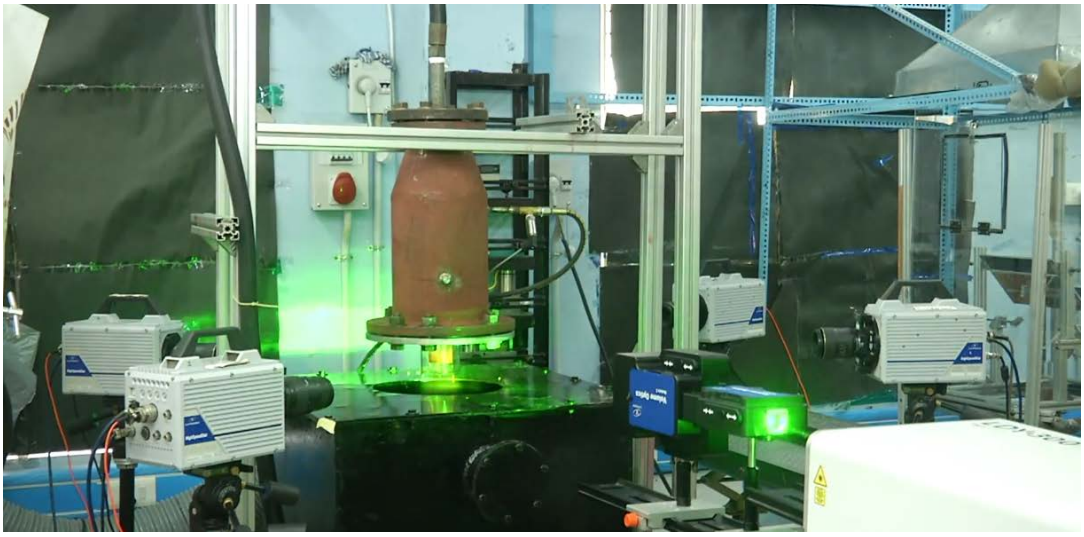

Figure 2. Example of an experimental setup arrangement

3. Results and discussion

Through the current section, results for measurements are represented and for each characteristic a comparisons between results for different flow rates are provided. Figure 3 shows the Seeded air flow downstream the injector.

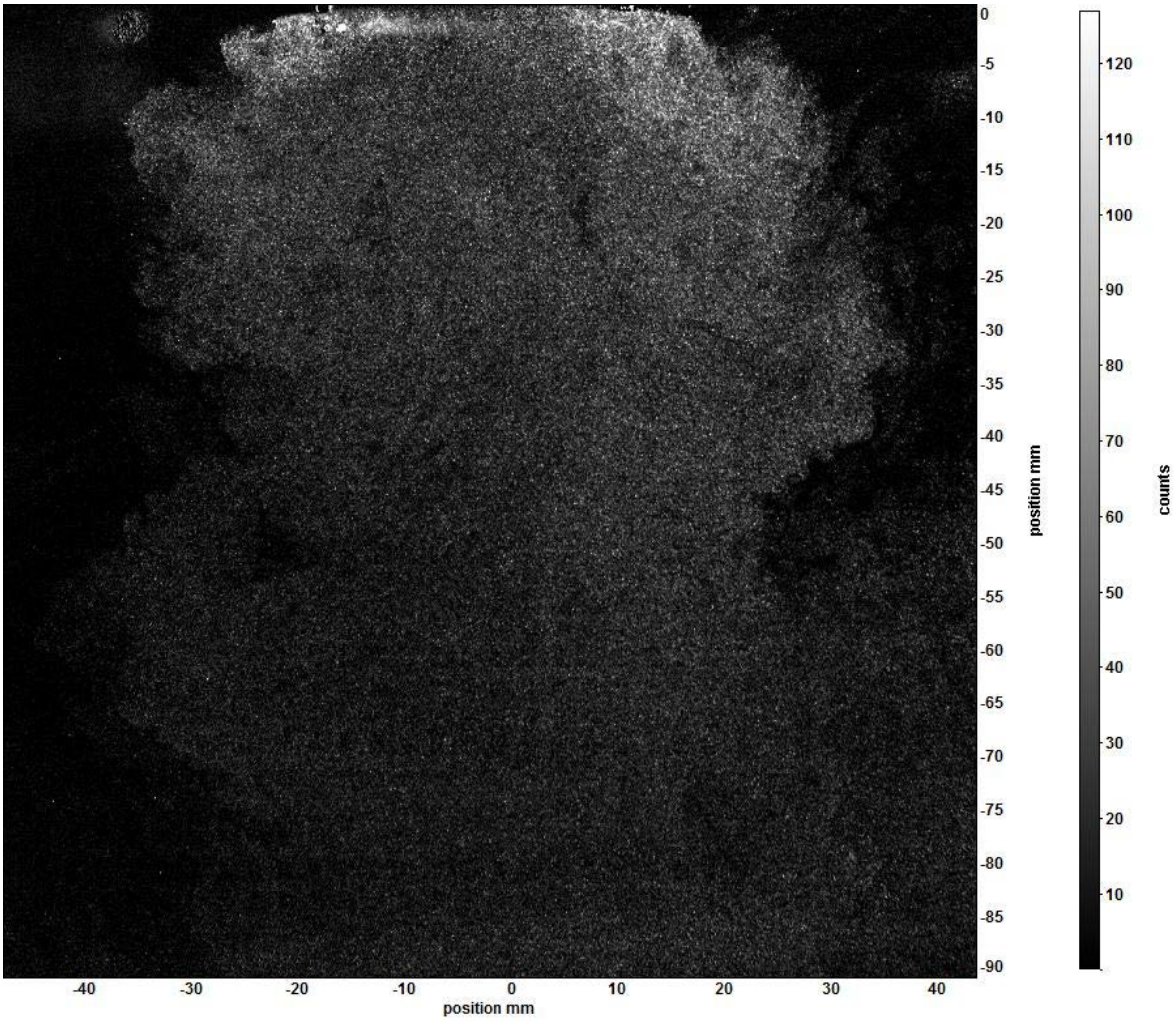

Figure 3. Seeded air flow downstream the injector.

3.1. Recirculation zone shape

From the results, CTRZ shape and dimensions for different flow rates are similar. In figure 4, symmetric configuration around a central vertical axis is clear. Width of the zone is approximately 34 mm while the height is approximately 37 mm. Moreover, for the different flow rates, results show almost independency on the air mass flow rate.

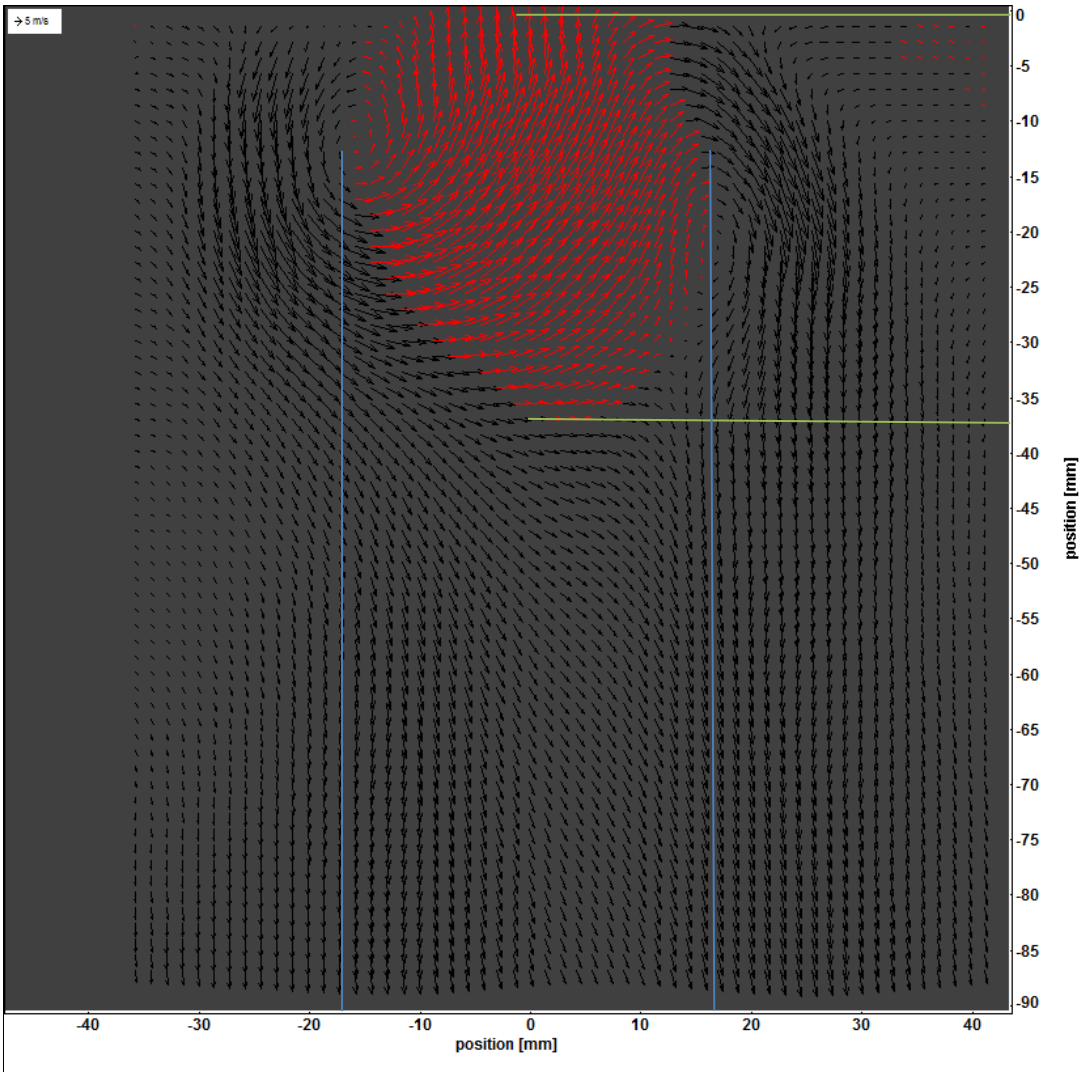

Figure 4. Recirculation zone for test case number 5.

3.2. Velocity field and shear strength

Velocity fields and shear strength for different test cases are shown in figure 5 and figure 6. As shown in the figures, velocity fields are similar in characteristics for the different test cases with change in velocity magnitude. Boundaries of the CTRZ have maximum shear strengths along with the largest velocity magnitudes. In addition, results show that increasing air mass flow rate increases the shear strength magnitude. CTRZs are indicated in the following figures by white circles while the boundaries of the CTRZs are indicated by white arrows.

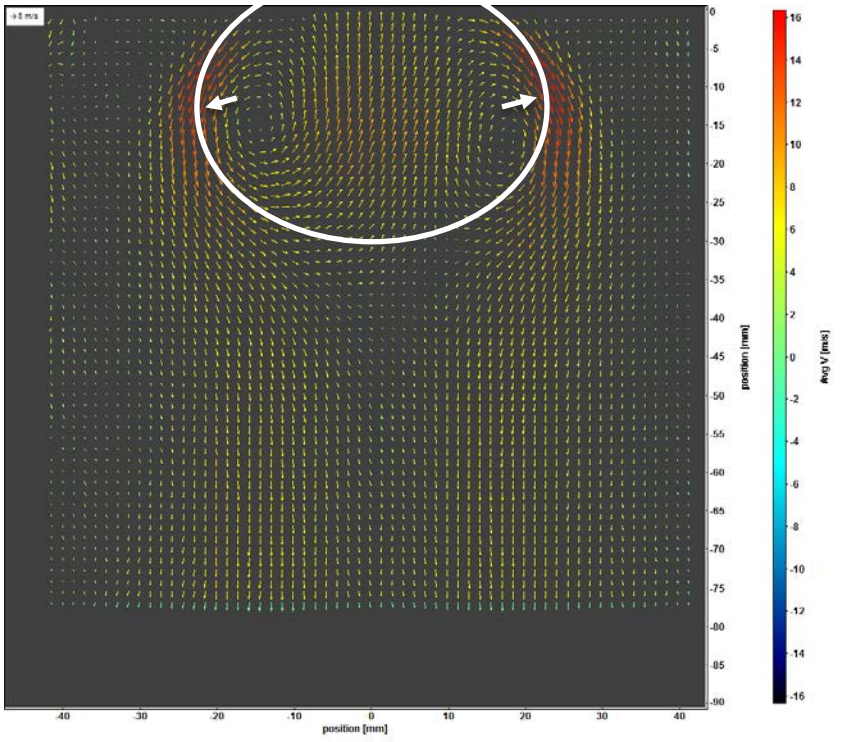

(a)

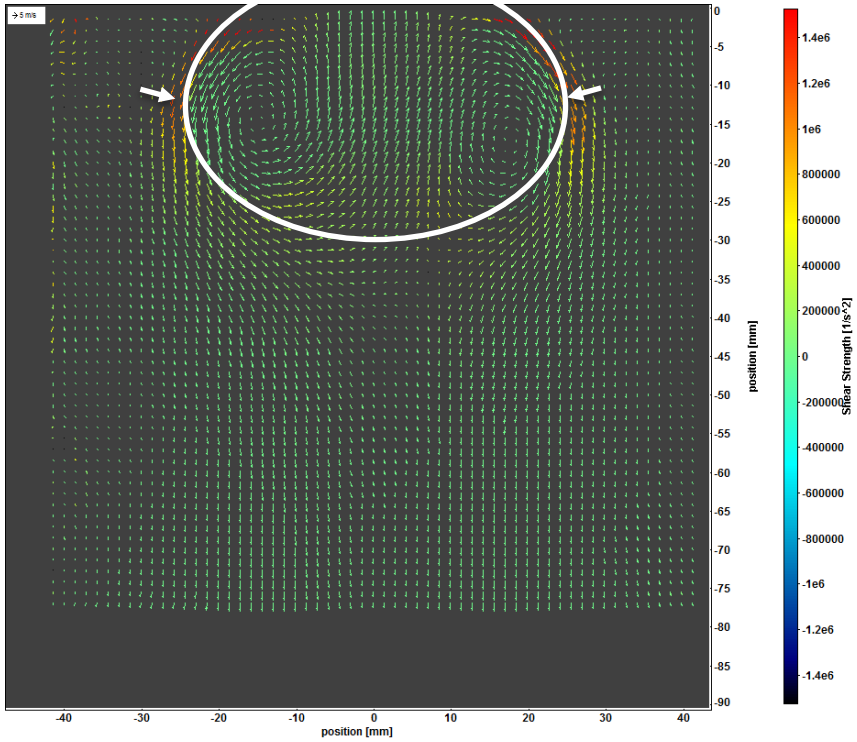

(b)

Figure 5. (a) Average velocity field for test case number 1, (b) Shear strength for test case number1.

The core region in figure 5 (a) has a velocity magnitude of 8 m/s while the maximum velocity is at the boundaries of the recirculation zone which is 16 m/s. The maximum shear strength in figure 5 (b) is $1.4*10^6$ ($1/s^2$) which is also at the boundaries of the recirculation zone.

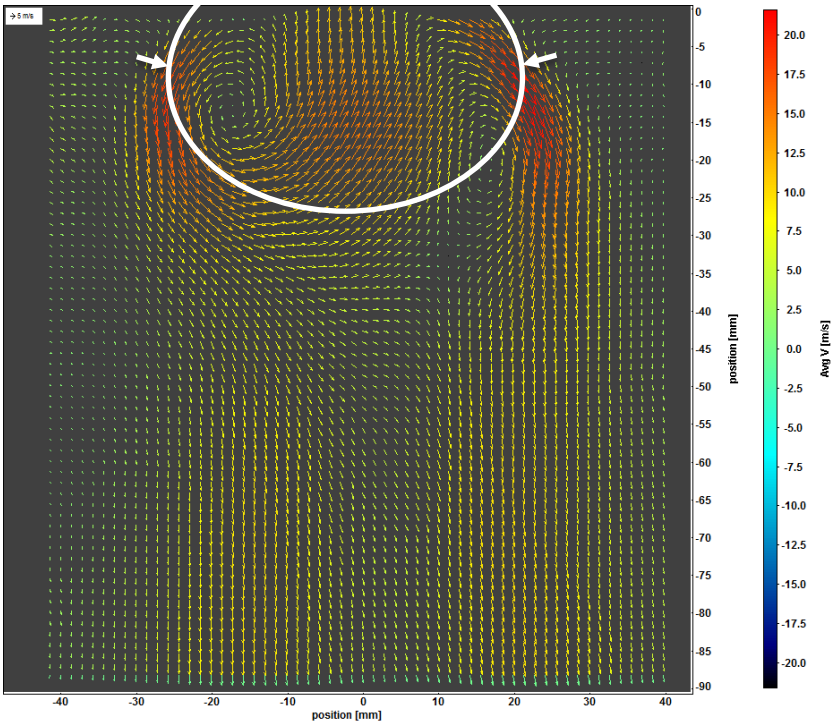

(a)

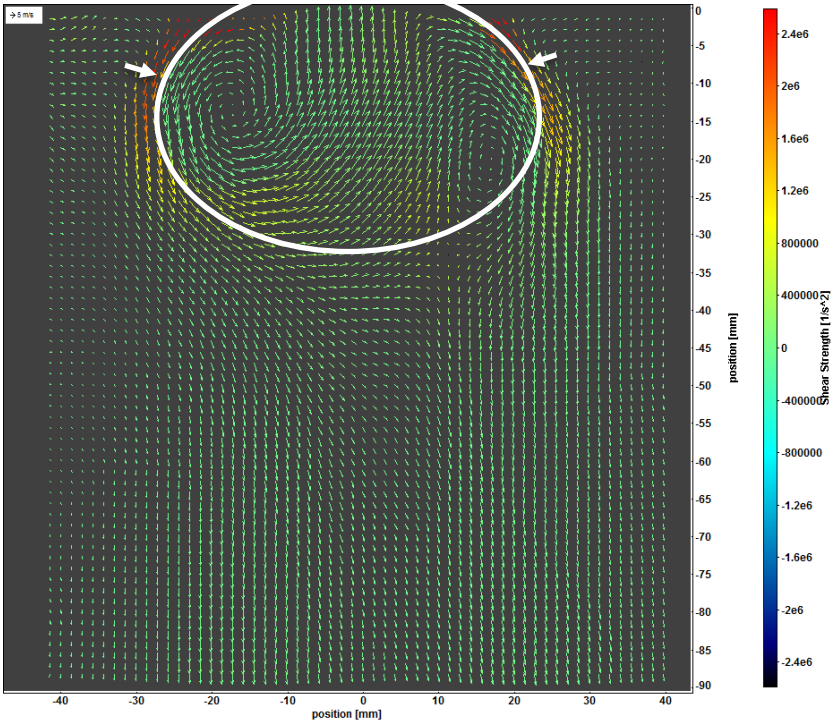

(b)

Figure 6. (a) Average velocity field for test case number 3, (b) Shear strength for test case number 3.

The core region in figure 6 (a) has a velocity magnitude of 14 m/s while the maximum velocity is at the boundaries of the recirculation zone which is 22 m/s. The maximum shear strength in figure 6 (b) is $2.4*10^6$ ($1/s^2$) which is also at the boundaries of the recirculation zone. The other test cases have similar results with same profile shapes but with differences in magnitudes.

3.3. V_y along a horizontal line

V_y along a horizontal line has similar profile shape for different flow rates with change in maximum velocity magnitudes at the core and at the boundaries of the CTRZ. Recirculation zone width can also be noticed as the region between points that cross the zero velocity line which has the same width similar to those results in the subsection 3.1.

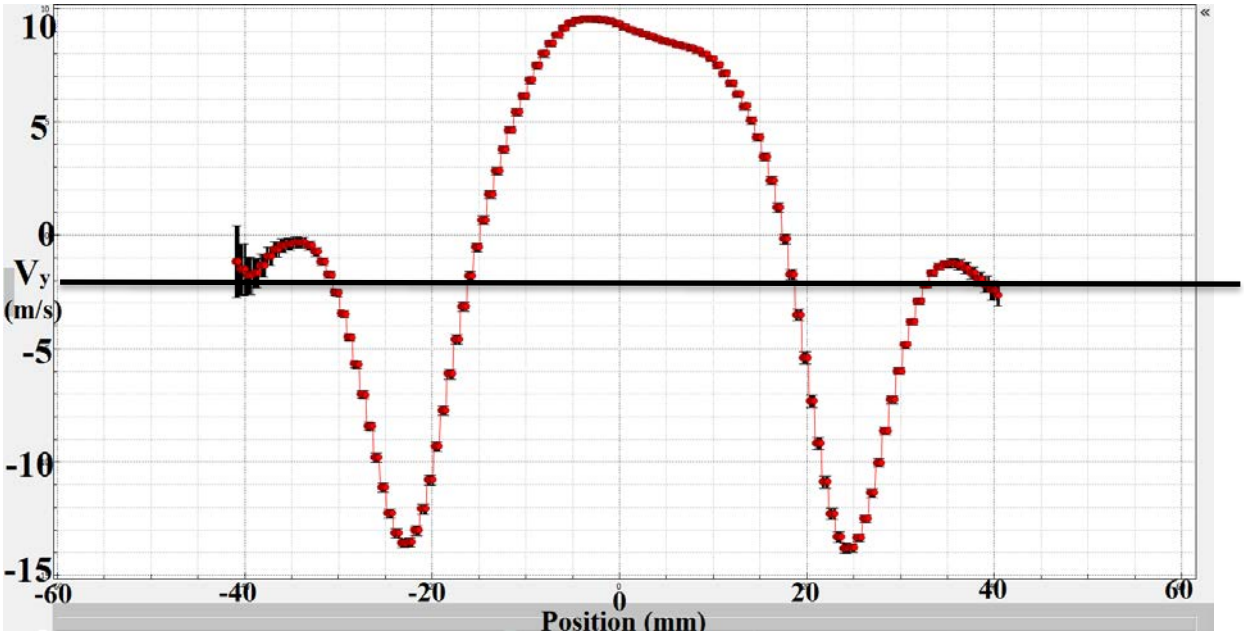

Figure 7. V_y along a horizontal line for test case number 1.

For the test case number 1 as shown in figure 7, the core has maximum velocity magnitude of 10 m/s while the CTRZ boundaries have magnitude of 14 m/s. Additionally, for the test case number 3, the core region has a maximum velocity magnitude of 14 m/s while the CTRZ boundaries have a magnitude of 19 m/s. The width of the CTRZ for both cases is around 34 mm. The other test cases have similar results with same profile shapes with same widths but with differences in velocity magnitudes.

4. Conclusion

Recirculation zone is formed by a toriodal flow in the region immediately downstream the injector. That flow has a significant effect in increasing combustion efficiency by mixing the fresh air and fuel downstream the injector with combustion products. Experimental investigation for recirculation zone characteristics is performed using a pre-filming airblast injector. Moreover, PIV is used for imaging the flow downstream the injector and the captured date is processed by a commercial software Davis. Olive oil is used as a tracer for its good characteristics in following the flow and in scattering the light. Results are represented for recirculation zone shape and geometrical characteristics, velocity field and shear regions. The shape of the CTRZ is found to be symmetrical about the central axis having the same dimensions for different test cases. Furthermore, the boundaries of the CTRZ have the maximum

velocity magnitudes and maximum shear strength values. Vy along a horizontal axis is found to have the same shape profile for various test cases with difference in maximum velocity magnitudes.

References

[1] Bahr D W 1996 *Unsteady combustion* (Dordrecht: Springer)
[2] Correa S M 1993 *Combustion science and technology*, **87(1-6)** pp 329-62
[3] Lefebvre A H 1999 *Gas Turbine Combustion, 2nd edition* (Philadelphia: Taylor & Francis)
[4] Han Y M, Seol W S, Lee D S, Yagodkin V I and Jeungm I S 2001 *Journal of Engineering for Gas Turbines and Power* **123(1)** pp 33-40
[5] Winterfeld G, Eickhoff H E and Depooter K 1990 *Design of modern gas turbine combustors* (San Diego: Academic Press)
[6] Hall M G 1972 *Annual review of fluid mechanics* **4(1)** pp 195-218
[7] Leibovich S 1978 *Annual review of fluid mechanics* **10(1)** pp 221-46
[8] Leibovich S 1984 *AIAA journal* **22(9)** pp 1192-1206
[9] Lucca-Negro O and O'doherty T 2001 *Progress in energy and combustion science*, **27(4)** pp 431-81
[10] Reddy A P, Sujith R I, and Chakravarthy S R 2006 *Journal of Propulsion and Power* **22(4)** pp 800-08
[11] Gupta A K, Lilley D G and Syred N 1984 *Swirl Flows* (Kent: Abacus Press)
[12] Beer J and Chigier N 1972 *Combustion Aerodynamics* (London: Applied Science Publishers LTD)
[13] Tangirala V, Chen R H and Driscoll J F 1987 *Combustion Science and Technology* **51(1-3)** pp 75-95
[14] Lu X, Wang S, Sung H G, Hsieh S Y and Yang V 2005 *Journal of Fluid Mechanics* **527** pp 171-95
[15] Candel S, Durox D, Schuller T, Bourgouin J and Moeck J P 2014 *Annual Review of Fluid Mechanics* **46 (1)** pp 147-73
[16] Kilik E 1985 *23rd Aerospace Sciences Meeting* pp 187
[17] Syred N and Beer J M 1974 *Combustion and flame* **23(2)** pp 143-201
[18] Hadef R and Lenze B 2008 *Chemical Engineering and Processing: Process Intensification* **47(12)** pp 2209-2217
[19] Wang S, Yang V, Hsiao G, Hsieh S and Mongia H C 2007 *Journal of Fluid Mechanics* **583** pp 99-122
[20] Merkle K, Haessler H, Büchner H and Zarzalis N 2003 *International Journal of Heat and Fluid Flow* **24(4)** pp 529-37
[21] Benjamin M A 2000 *Atomization and Sprays* **10** pp 427-38
[22] Lefebvre A H and McDonell V G 2017 *Atomization and sprays* (Boca Raton, FL: CRC Press)
[23] Engelbert C, Hardalupas Y and Whitelaw J H 1995 *Proceedings of the Royal Society of London Series A: Mathematical and Physical Sciences* **451** pp 189-229
[24] Rizkalla A and Lefebvre A H 1975 *Journal of Engineering for Gas Turbines and Power* **97(3)** pp 316-20
[25] Rizk N K and Lefebvre A H 1980 *Journal of Engineering for Gas Turbines and Power* **102** pp 706-10
[26] Shanmugadas K, Manuprasad E, Chiranthan R and Chakravarthy S 2020 *Proceedings of Combustion Institute* **000** pp 1-8
[27] Raffel M, Willert C, Werely S and Kompenhans J 2007 *Particle Image Velocimetry A Practical Guide* (Berlin Heidelberg, New York: Springer)
[28] Hanson R K 1988 *Symposium (International) on Combustion* **21(1)** pp 1677-91
[29] Wu Q, Ye Q and Meng G 2012 *Journal of Mechanical Engineering Science* **227(9)** pp 1927-37

Acknowledgment

I wish to acknowledge the National Centre for Combustion Research and Development (NCCRD) for giving me access to its facilities and for the experimental support and guidance provided to me by NCCRD team.